Organocopper triggered cyclization of conjugated dienynes via tandem S N 2'/Alder-ene reaction

Tanzeel Arif, Cyril Borie, Marion Jean, Nicolas Vanthuyne, Michèle Bertrand, Didier Siri, Malek Nechab

▶ **To cite this version:**

Tanzeel Arif, Cyril Borie, Marion Jean, Nicolas Vanthuyne, Michèle Bertrand, et al.. Organocopper triggered cyclization of conjugated dienynes via tandem S N 2'/Alder-ene reaction. Organic Chemistry Frontiers, 2018, 5 (5), pp.769-776. 10.1039/c7qo00288b . hal-02053476

HAL Id: hal-02053476
https://amu.hal.science/hal-02053476

Submitted on 7 Apr 2019

HAL is a multi-disciplinary open access archive for the deposit and dissemination of scientific research documents, whether they are published or not. The documents may come from teaching and research institutions in France or abroad, or from public or private research centers.

L'archive ouverte pluridisciplinaire **HAL**, est destinée au dépôt et à la diffusion de documents scientifiques de niveau recherche, publiés ou non, émanant des établissements d'enseignement et de recherche français ou étrangers, des laboratoires publics ou privés.

Organocopper triggered cyclization of conjugated dienynes *via* tandem S_N2'/Alder-ene reaction†

Tanzeel Arif,[a] Cyril Borie,[a] Marion Jean,[b] Nicolas Vanthuyne,[b] Michèle P. Bertrand,[a] Didier Siri *[a] and Malek Nechab *[a]

Propargylic carbonates were converted to indenes through a S_N2'/Alder-ene cascade triggered by organocopper reagents. The reaction tolerates different organocopper species generated either from organolithiums or Grignard reagents. A catalytic version of this strategy could be devised using either copper or iron catalysts. Attempts to transfer chirality from an enantioenriched substrate revealed a moderate chirality conversion because of a low discrimination between the two faces of the internal olefinic partner with these typical substrates. The theoretical investigation supports a concerted closed-shell mechanism and highlights the influence of the substituents on the activation parameters and on the synchronicity of C–H bond breaking and C–C bond forming during the Alder-ene step.

Introduction

Cascade or domino reactions are powerful to introduce molecular complexity *via* multibond formation. In this context cycloisomerizations of polyenes and enynes have found an ever-increasing number of synthetic applications.[1] Among carbocycles, indenes constitute an important class of compounds that possess interesting biological activities. For example, the methylindene in Scheme 1b, an analogue of our targeted molecules, has been reported to exhibit antidepressant properties.[2] In addition, they are useful precursors of chiral ligands for asymmetric synthesis.[3] The elaboration of the indenyl framework through cascade reactions has been the matter of numerous reports.[4]

Recently, we have focused our efforts on enantioselective cascade rearrangements of enediynes implying the memory of a chirality phenomenon.[5] Following on from this study, a new strategy leading to benzofulvenes through a bis-alkylating cycloisomerization of enediynes involving a double transfer of chirality has been developed (Scheme 1a).[6,7] This methodology was then implemented to propose a chemo-, diastereo- and enantioselective access to chiral indenes from conjugated dienynes bearing a Michael acceptor (Scheme 1a).[8] Both strategies relied on the use of the stereo-controlled S_N2' displacement of an enantiopure propargylic carbonate by a dialkylcuprate to generate *in situ* a transient chiral allenic motif. In line with these studies, it was natural to investigate the scope of the tandem alkylation/Alder-ene rearrangement of dienynes triggered by organocopper reagents as a potential route to isopropenylindenes according to Scheme 1b. In parallel, we have devised a Pd-catalyzed diastereoselective synthesis of indenes bearing a chiral axis and a stereocenter.[9]

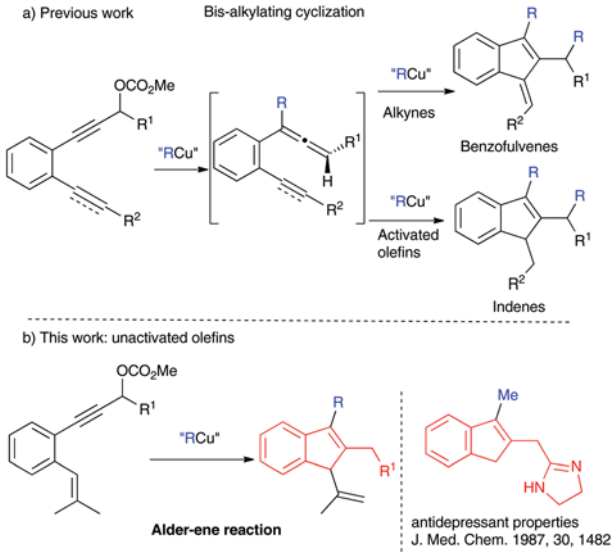

Scheme 1 Formation of indenes from conjugated enediynes and dienynes.

Results and discussion

Allenes are known as activated enophiles.[10] Despite the fact that Alder-ene cyclizations have rather high activation barriers

[a]*Aix-Marseille Univ, CNRS, ICR, Marseille, France.*
E-mail: malek.nechab@univ-amu.fr, didier.siri@univ-amu.fr
[b]*Aix-Marseille Univ, Centrale Marseille, CNRS, iSm2, Marseille, France*

and are most often performed at temperatures above 100 °C,[11,12] the reaction of organocuprates with propargyl carbonate **1a** bearing an isopropylidene moiety afforded the expected indenes **3aa–3ah** at room temperature. Structural diversity could be introduced by varying the nature of the organocopper reagent (Table 1). Methyl, *n*-butyl, *i*-butyl, phenyl, *i*-propyl, ethyl and $TMSCH_2$ groups could be incorporated easily with yields varying from 55 to 67% through this two-step cascade process.[13] However, when a bulky *t*-butyl cuprate was used, allene **2ae** was isolated as the only product (Table 1, entry 5). The latter was shown to slowly evolve to indene **3ae** upon heating at 60 °C (70% conversion after 6 h). It is worth noting that the introduction of an additional phenyl group stabilized the intermediate allene **2af** so that its conversion was incomplete under the standard conditions. The conversion into **3af** could however be completed within 24 h at room temperature. The quenching of the reaction implying $Me_2CuLi{\cdot}DMS$ after 5 minutes at −20 °C also confirmed that allene **2** was the key intermediate in this process; a 95 : 5 mixture of allene **2aa** and indene **3aa** was isolated in 64% yield under these experimental conditions (Table 1, entry 10).

The copper-catalyzed synthesis of allenes from propargylic electrophiles and Grignard reagents has been reported.[14] Under these conditions (Table 1, entry 8, conditions **C**), indene **3ag** was isolated in 56% yield. This result opens interesting prospects for the development of an asymmetric version of the process by making use of chiral ligands. An elegant synthesis of allenes which used a stoichiometric Grignard reagent and catalytic $Fe^{(III)}$ (1 mol%) was published by Bäckvall.[15] By analogy with the copper mediated reaction, an *in situ* generated organoiron species is supposed to be promoting the S_N2' displacement of a propargyl acetate. This protocol was applied to substrate **1a** that was allowed to react with MeMgBr and $FeCl_3$ (5 mol%). The non-optimized reaction afforded product **3aa** in 46% yield.

The scope and limitations of the reaction were examined under conditions **A** or **B** (Scheme 2). The presence of an exocyclic double bond like in substrate **1b** was shown to be compatible with the Alder-ene process. Additionally, the pyridine scaffold in **1c** was tested with success, as it could offer interesting prospects for potential application of the resulting indenes in catalysis. However, the overall yield was lower in this case. This might be explained by the ability of the pyridine unit to complex with copper.

The nature of the substituent on the terminal position of the allenic moiety introduces a limitation to the cyclization step. When the phenyl group at the propargylic position was replaced by a methyl group (**1d**), allene **2dg** was the unique product of the reaction isolated in 55% yield. The latter could not be further cycloisomerized into **3dg** and remained the only product, even when the reaction was performed in THF at reflux over 1 h (Scheme 2). The same behavior was observed with substrate **1e**; allene **2ec** did not evolve to indene. These two experiments suggest that the phenyl group is crucial to the success of the Alder-ene step.

The aromatic ring at the propargylic position was tolerant to fluorine substitution as the indenes **3fb** and **3fg** were isolated with 46% and 49% yields, respectively. The series could not be expanded to aryl groups bearing electron-donating substituents. A methoxy-substituted substrate was tentatively synthesized. It turned out to be unstable. This is likely to be due

Table 1 Organocopper reagent scope

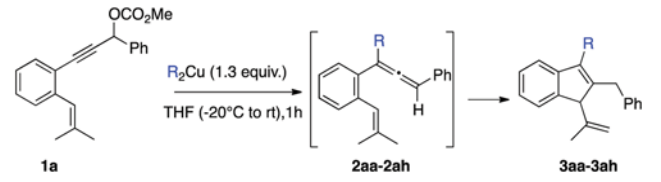

Entry	R	Procedure[a]	2 : 3 (NMR ratio)	Yield
1	Me (**a**)	**A**	**2aa/3aa** (0 : 100)	55
2	Bu (**b**)	**A**	**2ab/3ab** (0 : 100)	57
3	*i*-Bu (**c**)	**A**	**2ac/3ac** (0 : 100)	60
4	$TMSCH_2$ (**d**)	**A**	**2ad/3ad** (0 : 100)	58[b]
5	*t*-Bu (**e**)	**A**	**2ae/3ae** (97 : 3)	61
6	Ph (**f**)	**B**	**2af/3af** (25 : 75)	56[b]
7	*i*-Pr (**g**)	**B**	**2ag/3ag** (0 : 100)	67
8	*i*-Pr (**g**)	**C**	**2ag/3ag** (0 : 100)	56
9	Et (**h**)	**B**	**2ah/3ah** (0 : 100)	67
10	Me (**a**)	**B**[c]	**2aa/3aa** (95 : 5)	64

[a] Conditions **A**: A THF solution of $R_2Cu{\cdot}LiBr$ (prepared from 2.6 equiv. of RLi and 1.3 equiv. of CuBr·DMS) was added dropwise to a solution of enyne **1a** at −20 °C, and then the reaction mixture was allowed to warm to rt for 1 h. Conditions **B**: A THF solution of $R_2Cu{\cdot}MgX$ (prepared from 2.6 equiv. of RMgX and 1.3 equiv. of CuBr·DMS) in THF was added dropwise to a solution of dienyne **1a** at 0 °C and then the reaction mixture was allowed to warm to rt for 1 h. Conditions **C**: 2.6 equiv. of *i*-PrMgCl and only 20 mol% of CuBr·DMS were used. [b] 4 h were needed to complete the reaction. [c] After 5 minutes at −20 °C, the reaction was stopped.

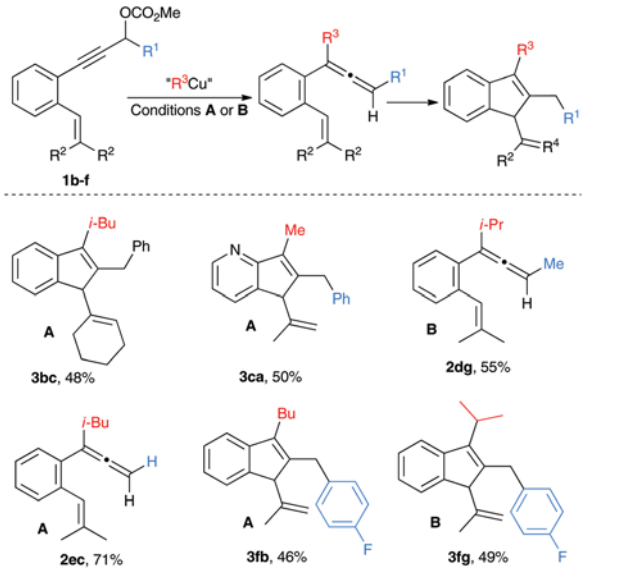

Scheme 2 Scope and limitations.

to the rather easy formation of a carbocation at the propargylic position.

Computational study

In order to gain more insight about the parameters controlling the Alder-ene step, we performed theoretical calculations at the M06-2X/6-311++G(3df,3pd)//M06-2X/6-31G(d) level of theory in the gas phase. The goal was to determine which of the three possible pathways leading from allenes **2** to indenes **3** was the most likely (Scheme 3).[16,17] Optimized stationary points were characterized as minima (no imaginary frequency) or transition states (one imaginary frequency) by computing the corresponding vibration frequencies. All transition state geometries were confirmed by IRC calculations. The calculated values for the activation enthalpy, the activation free energy and the exothermicity of the reaction are reported in Table 2.

Three hypotheses were examined, *i.e.*, the concerted closed-shell mechanism (path a), the biradical ring closure followed by 1,5-hydrogen atom abstraction (HAT) (path b) and the two-step polar mechanism (path c) (Scheme 3).[18]

The possibility of two alternative mechanisms had previously been addressed by several authors for the Schmittel cyclization of conjugated enyne-allenes (concerted and diradical routes),[19] and the incidence of substituent effects on the preferred route was investigated. Due to the observed impact of introducing a phenyl group at the terminal carbon of the allene, both radical and polar two-step mechanisms (paths b and c) were envisaged as alternatives to the concerted route (path a) in the case of the rearrangement of conjugated diene-allenes.

The comparison of the first two routes was achieved in the typical cases of allenes **2aa** and **2dg**; the polar path was examined only in the case of **2aa**.

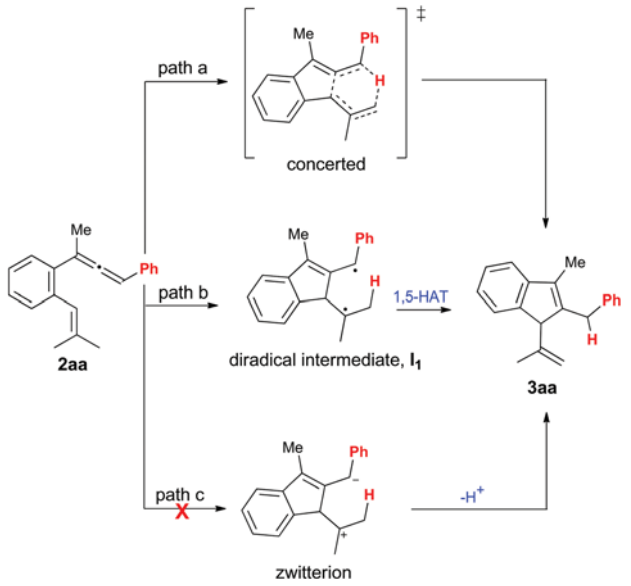

Scheme 3 Possible pathways for the rearrangement of conjugated diene-allenes.

Table 2 Computed activation enthalpies, activation free energies and enthalpies of the reaction at the (U)M06-2X/6-311++G(3df,3pd)//(U)M06-2X/6-31G(d) or (U)CCSD(T)/cc-pVDZ //M06-2X/6-31G(d) levels of theory

Entry	Allene (R, R^1)	$\Delta H^{\#}$	$\Delta G^{\#}$	ΔH_r
1	**2aa** (Me, Ph)	26.1 [29.9, 27.5][a]	27.5 [31.3, 28.9][a]	−27.2
2	**2aa** [b]	21.4 [34.5]	22.8 [35.9]	−31.7
3	**2ab** (*n*-Bu, Ph)	25.8	27.2	−27.5
4	**2ac** (*i*-Bu, Ph)	24.9	26.2	−29.2
5	**2ac** [b]	19.7	21.0	−33.8
6	**2ae** (*t*-Bu, Ph)	29.9	31.1	−21.2
7	**2af** (Ph, Ph)	28.8	30.7	−25.9
8	**2ag** (*i*-Pr, Ph)	27.7	29.8	−23.5
9	**2dg** (*i*-Pr, Me)	29.8 [35.2, 32.4][a]	32.7 [36.7, 33.9][a]	−26.5
10	**2ec** (*i*-Bu, H)	26.9	29.6	−33.3

[a] The values of the uncorrected and spin-corrected activation parameters of the rate determining step of the diradical pathway at the UM06-2X/6-311++G(3df,3pd)//UM06-2X/6-31G(d) are given in that order in brackets. [b] Energy values calculated at the (U)CCSD(T)/cc-pVDZ//(U)M06-2X/6-31G(d) levels.

In order to obtain comparable energy values, the diradical route was first computed at the same level as the closed-shell mechanisms, using the broken spin symmetry unrestricted theory (UM06-2X/6-311++G(3df,3pd)//UM06-2X/6-31G(d)). As regard to the description of the transition state, it must be noticed that low spin contamination was registered (the $<S^2>$ value for the spin contaminated wave function was 0.3 in both cases, as opposed to the ideal values of zero for pure singlet states and 2 for triplets). Wave functions were spin-unrestricted stable. Empiric corrections to pure singlet are reported in Table 2; spin projected values were calculated using the Yamaguchi and Houk procedure.[20]

The two-step radical profile was fully computed in order to ensure that the formation of the biradical was the rate determining step. The $\Delta G^{\#}$ value for the cyclization step was indeed found to be nearly 12 kcal mol^{-1} higher than that of the ensuing hydrogen atom migration, which furthermore should be accelerated by the tunneling effect.[21] Only the activation parameters for the rate limiting step leading to the diradical are given in brackets in Table 2 in entries 1 and 2 for **2aa**, and in entry 9 for **2dg**.

The concerted route (Table 2, entry 1) was found favored over the diradical pathway by only 1.4 kcal mol^{-1} (spin-corrected value) at the M06-2X/6-311++G(3df,3pd)//M06-2X/6-31G(d) level. This made it difficult to rule out the diradical route when one out of the two incoming radical centers is stabilized by a phenyl group.

In the case of **2dg** (Scheme 2) the gap between the two activation barriers was larger (2.6 kcal mol^{-1}, Table 2, entry 9). Nevertheless, considering that the activation energy difference between the two paths is lowered by the empiric correction (from 3.8 to 1.4 kcal mol^{-1} in the case of **2aa** and from 5.4 to 2.6 kcal mol^{-1} in the case of **2dg**) we inclined to favor path a as the preferred one.

The M06-2X functional is recommended most highly for the study of main-group thermochemistry and kinetics.[16]

However, the calculated activation barriers were obviously overestimated in light of the effective reaction times.[22a,b] High accuracy methods like CBS-QB3 or G3B3 are not adapted to the size of our molecules (number of atoms ≥40). In order to improve the computed values of the activation parameters, the energies of the stationary points were recalculated at the CCSD (T)/cc-pVDZ level of theory from the geometries optimized at the M06-2X/6-31G(d) level. These values are given in Table 2, entry 2 for **2aa**. They are clearly better consistent with the experimental data. According to the (U)CCSD(T)/cc-pVDZ//(U) M06-2X/6-31G(d) computed activation free energies, the barrier for the first step of the radical route (35.9 kcal mol^{-1}) is much higher than the barrier for the concerted rearrangement (at this level of theory, the activation free energy for the second step is 19.0 kcal mol^{-1}), which confirms that the cyclization step is rate limiting. These data support the conclusion that the concerted path a is favored over the two-step path b.

The comparison between the concerted[23] and diradical routes is exemplified in Fig. 1, the typical case of **2aa** which is the smallest element in the series of substrates.

Due to the charge stabilizing effect of the phenyl group, the eventuality of a two-step polar pathway (Scheme 3, path c) remained to be examined in order to better cover the energy potential surface of the rearrangement. The latter route was examined in the case of allene **2aa**. No zwitterionic intermediate could be found as a possible energy minimum at the restricted M06-2X/6-311++G(3df,3pd)//M06-2X/6-31G(d) level of theory. Instead, two valence isomers of the starting compound were found as energy minima, and they are shown in Fig. 2. The first one $\mathbf{I_2}$ has a tricyclic structure with a distorted three-membered ring. Its enthalpy is superior by 1.3 kcal mol^{-1} to that of **2aa**. However, no transition states could be found either backward to the substrate or forward to the product from this structure. The second valence isomer $\mathbf{I_3}$ could, like the former, conceptually derive from a polar closure of the five-membered ring (Scheme 3). It could also result from a formal concerted intramolecular [4 + 2]-cycloaddition. It is more stable by 19.9 kcal mol^{-1} than **2aa**. The transition state **TS3** (Fig. 2) corresponding to a 31.1 kcal mol^{-1} activation enthalpy was found on the pathway leading from **2aa** to $\mathbf{I_3}$. It is 5.0 kcal mol^{-1} higher than the activation energy calculated for the concerted route at the same level. Moreover, no route could be found forward from $\mathbf{I_3}$ to **3aa**. Thus, it can be concluded that none of the two valence isomers are intermediates in the transformation of **2aa** into **3aa**.

In order to discuss the substituent effect, computational data for the concerted pathway were extended to the whole series. These data were computed at the less time-consuming level of theory. We observed that the IRC descents backward (from TS to reactant) and forward (from TS to product) led to the most stable conformers of these latter in all but two cases (Table 2, entries 6 and 8). In the case of **2ag**, the product was further optimized to take into account its most stable conformation and correct the reaction enthalpy. In the case of **2ae**, the reactive conformation of the allene (optimized after IRC) was shown to be less stable by 2.3 kcal mol^{-1} than the ground state conformer. A rotational barrier of 8.2 kcal mol^{-1} must be passed to reach the conformer prone to undergo the concerted Alder-ene cyclization (the corrected reaction enthalpy and activation parameters are given in Table 2).

As an additional argument in support to the validity of the discussion based on relative energies calculated at the M06-2X/6-311++G(3df,3pd)//M06-2X/6-31G(d) level, it can be pointed out that the activation parameters, calculated for **2aa** and **2ac** at the CCSD(T)/cc-pVDZ//M06-2X/6-31G(d) level, vary in the same way as the values calculated at the former level (entries 1 and 4/entries 2 and 5).

The examination of the transition state structures shows that the concerted process is rather asynchronous. In the transition state, the forming of the indene C–C bond is significantly more advanced than the breaking of the C–H bond at least for **2aa–2ag**. The valence angles of the central carbon atom of the allene are much closer to those of the sp^2 hybridized C atom of the indene ring and conversely, the proximal carbon atom of the double bond is significantly pyramidalized in the transition states (Table 3). It is worth noting that the C–H bond which is broken (C5–H6) is already slightly weakened due to the overlap between the π orbital of the double bond and the σ* orbital of the C–H bond (see Fig. 1 for the atom numbering).

It has already been observed that the more asynchronous the reaction is, the lower is the activation barrier.[17] This would be consistent with the rather high activation barriers calculated for the rearrangement of allenes **2dg** and **2ec**. The computed C2–C4 and C5–H6 bond lengths are both longer in the corresponding transition states in these two cases (Table 3).

The slowing down of the concerted Alder-ene reaction at room temperature in these latter cases seems to be consistent with the progress of the reaction in terms of C–C bond formation and C–H bond breaking which are a bit different from the other allenes in the series. The examination of interatomic distances confirms that the more distant are C_2 from C_4 and C_3 from H_6 in the allene, the slower the concerted Alder-ene process. With respect to these parameters, the reactivity of **2af** fits well in the series. The theoretical study correlates the observed reactivity trend to structural parameters.

Transfer of chirality

As enantioenriched propargyl carbonates can be prepared easily from commercially available propargylic alcohols, we have endeavored to promote a double transfer of chirality from (*R*)-**1a** to extend the access to enantioenriched indenes (Scheme 4).[24] Despite the lack of discrimination between the two diastereomeric transition structures in the case of the rearrangement of allene **2aa**,[23] a cascade involving central-to-axial-to-central chirality transfer was achieved with an encouraging 55% recovery of the original ee when reacting (*R*)-**1a** with *i*-Bu_2Cu.

Attempts to improve the chirality transfer by changing experimental conditions like temperature, solvent and reac-

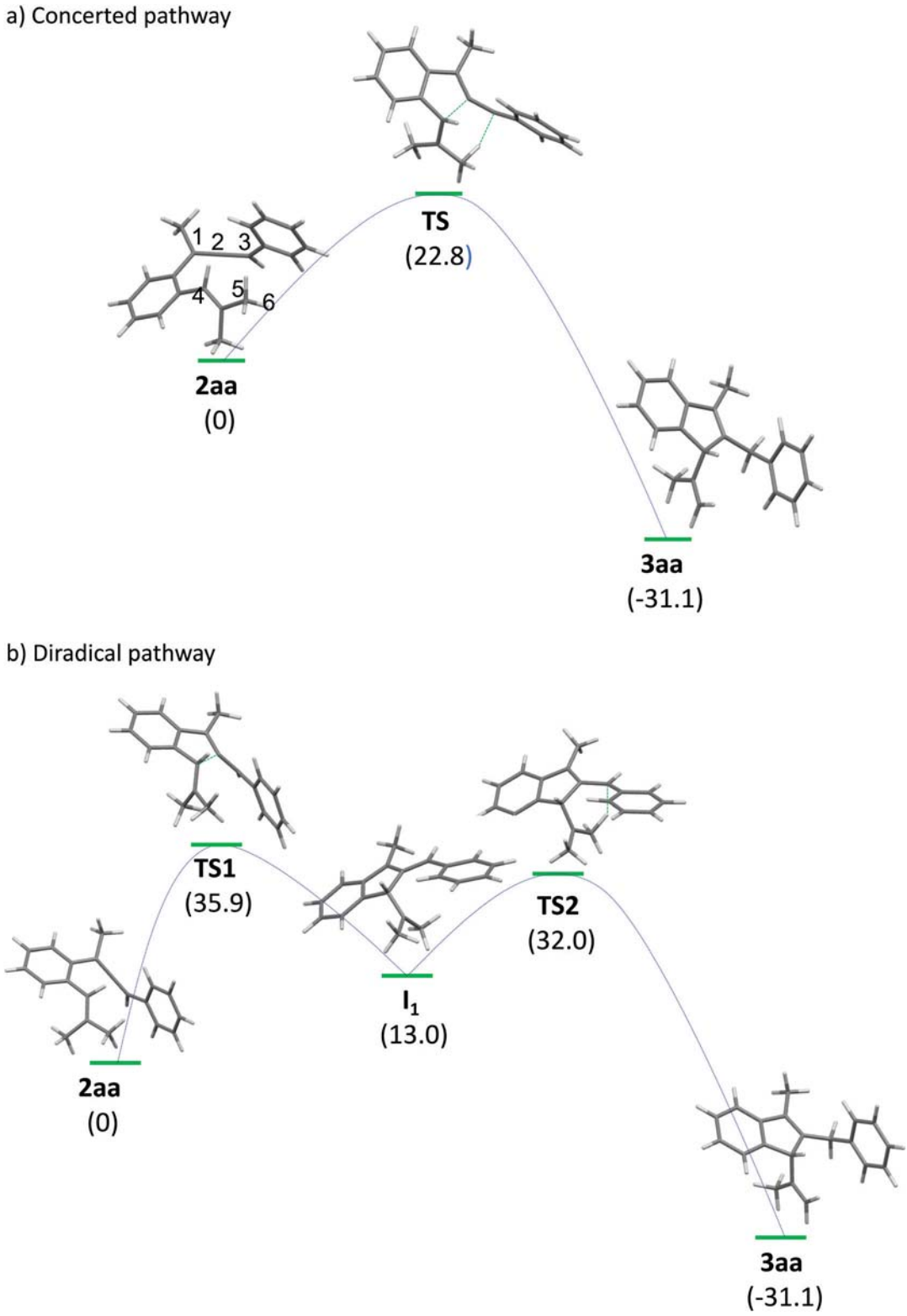

Fig. 1 Typical energy profiles for the concerted (a) and the two-step biradical pathway (b) in the case of **2aa** (the values in the parentheses are the relative free energies in kcal mol^{-1} calculated at the (U)CCSD(T)/cc-pVDZ//M06-2X/6-31G(d) level of theory).

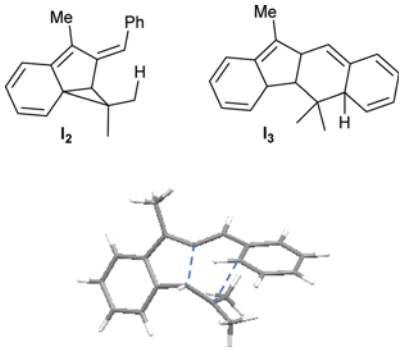

Fig. 2 Structures of valence isomers I_2 and I_3 and transition state **TS3**.

Table 3 Evolution of interatomic distances and valence angles: extent of C–H bond breaking/forming, and C–C bond forming in the transition state of the concerted pathway (see, Fig. 1 for the atom numbering)

	C_4–C_2 (Å)	C_5–H_6 (Å)	C_3–H_6 (Å)	C_1–C_2–C_3 valence angle
2aa	2.881	1.096	3.952	179.7°
2aa-TS	1.850	1.190	1.782	140.0°
3aa	1.522	3.417	1.099	129.2°
2ab	2.875	1.098	3.961	178.7°
2ab-TS	1.851	1.191	1.784	139.7°
3ab	1.522	3.344	1.099	128.9°
2ac	2.852	1.098	3.907	178.2°
2ac-TS	1.849	1.199	1.757	139.4°
3ac	1.520	3.435	1.099	129.0°
2ae	3.199	1.096	4.723	178.3°
2ae-TS	1.864	1.199	1.74	142.2°
3ae	1.523	3.062	1.099	133.0°
2af	2.988	1.098	3.954	178.9°
2af-TS	1.850	1.190	1.782	140.0°
3af	1.522	3.410	1.099	128.9°
2ah	2.969	1.098	3.968	179.4°
2ah-TS	1.858	1.210	1.711	140.7°
3ah	1.524	3.089	1.099	120.0°
2dg	3.014	1.09	4.237	178.0°
2dg-TS	1.979	1.258	1.588	146.3°
3dg	1.526	3.118	1.097	132.0°
2ec	3.046	1.097	5.110	179.5°
2ec-TS	1.987	1.256	1.608	145.2°
3ec	1.522	3.514	1.098	128.8°

tants were unsuccessful. It was previously demonstrated that the experimental conditions were suitable for the formation of enantioenriched allenes.[14] Therefore, the loss of ee necessarily results from the cyclization step.

The low discrimination, between the two faces of the double bond in the transition structure of the cyclization, is the main limitation to the chirality transfer. Theoretical calculations confirmed this assumption. In the case of **2ac**, the transition states involving the *re* and the *si* faces of the double bond exhibit only 1.3 kcal mol^{-1} difference, which is in fair agreement with the observed decrease of the ee (Scheme 4). Taking into account the difficulty in controlling the selective synthesis of substrates bearing *E* or *Z* alkenes, and the risk that the introduction at the distal sp^2 carbon of one or two different alkyl substituents other than methyl (with the exception of CH_2TMS and related bulky groups) might result in the formation of mixtures of regio-isomers and of *E* and *Z* stereoisomers of the product,[10] we decided not to continue our efforts in this direction. Instead, concomitant studies making use of chiral cycloalkylidenes to control chirality transfer in the same type of cascading rearrangement proved to be successful.[25]

Conclusions

The S_N2' displacement of propargylic carbonates by dialkyl cuprates followed by intramolecular Alder-ene cyclization provides indene frameworks bearing an alkylidene substituent. The present study has highlighted the scope and limitations of this cascade process that tolerates various organocopper species generated either from organolithium or Grignard reagents. The theoretical investigation of the intramolecular Alder-ene step supports the concerted nature of the rearrangement. It enlightens the influence of the substituents on the activation parameters and on the synchronicity of C–H bond breaking and C–C bond forming during this key step. Moreover, the computed activation free energies have confirmed that the facial approach of the olefin partner in the

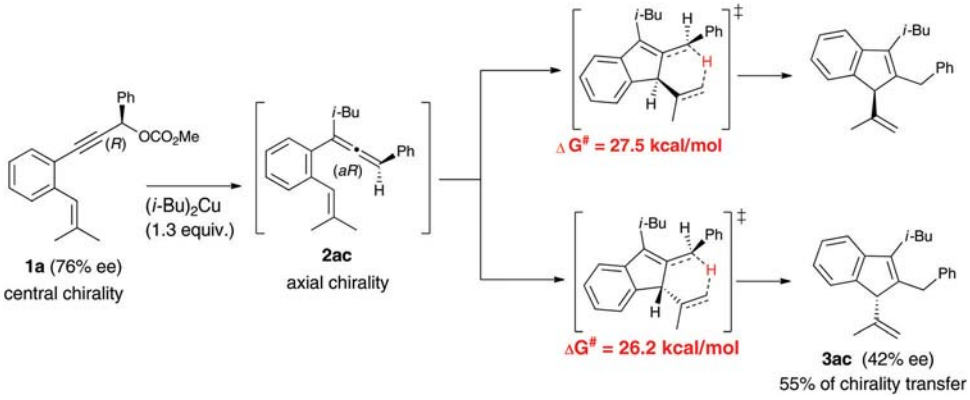

Scheme 4 Tentative of chirality transfer from enantioenriched **1a**.

cyclization step is not discriminative enough, which affects the degree of chirality transfer with this type of substrate.

Acknowledgements

We thank Aix-Marseille Université and CNRS for financial support. We also thank Christophe Chendo and Valérie Monnier for MS analyses. This work was supported by the computing facilities of the CRCMM, "Centre Régional de Compétences en Modélisation Moléculaire de Marseille".

Notes and references

1 (*a*) For selected reviews see: Y. Zhu, L. Sun, P. Lu and Y. Wang, *ACS Catal.*, 2014, **4**, 1911–1925; (*b*) Y. Deng, A. K. Å. Persson and J.-E. Bäckvall, *Chem. – Eur. J.*, 2012, **18**, 11498–11523; (*c*) S. Mondal, M. P. Bertrand and M. Nechab, *Angew. Chem., Int. Ed.*, 2013, **52**, 809–811.

2 M. P. Wentland, D. M. Bailey, E. J. Alexander, M. J. Castaldi, R. A. Ferrari, D. R. Haubrich, D. A. Luttinger and M. H. Perrone, *J. Med. Chem.*, 1987, **30**, 1482–1489.

3 For a review see: C. Borie, L. Ackermann and M. Nechab, *Chem. Soc. Rev.*, 2016, **45**, 1368–1386.

4 For reviews see: (*a*) B. Gabriele, R. Mancuso and L. Veltri, *Chem. – Eur. J.*, 2016, **22**, 5056–5094; (*b*) M. Enders and R. Baker, *Curr. Org. Chem.*, 2006, **10**, 937–953; (*c*) For a selected example on indene synthesis involving Alder-ene reaction see: R. Sanz, A. Martínez, P. García-García, M. A. Fernández-Rodríguez, M. A. Rashid and F. Rodríguez, *Chem. Commun.*, 2010, **46**, 7427–7429.

5 (*a*) M. Nechab, D. Campolo, J. Maury, P. Perfetti, N. Vanthuyne, D. Siri and M. P. Bertrand, *J. Am. Chem. Soc.*, 2010, **132**, 14742–14744; (*b*) C. Campolo, A. Gaudel-Siri, S. Mondal, D. Siri, E. Besson, N. Vanthuyne, M. Nechab and M.P. Bertrand, *J. Org. Chem.*, 2012, **77**, 2773–2783.

6 D. Campolo, T. Arif, C. Borie, D. Mouysset, N. Vanthuyne, J.-V. Naubron, M. P. Bertrand and M. Nechab, *Angew. Chem., Int. Ed.*, 2014, **53**, 3227–3231.

7 For a recent review on chirality transfer see: D. Campolo, S. Gastaldi, C. Roussel, M. P. Bertrand and M. Nechab, *Chem. Soc. Rev.*, 2013, **42**, 8434–8466.

8 T. Arif, C. Borie, A. Tintaru, J.-V. Naubron, N. Vanthuyne, M.P. Bertrand and M. Nechab, *Adv. Synth. Catal.*, 2015, **357**, 3611–3616.

9 C. Borie, N. Vanthuyne, M. P. Bertrand, D. Siri and M. Nechab, *ACS Catal.*, 2016, **6**, 1559–1564.

10 (*a*) T. J. J. Müller, in *Comprehensive Organic Synthesis II*, Elsevier, 2014, pp. 1–65; (*b*) K. M. Brummond and A. Loyer-Drew, in *Comprehensive Organometallic Chemistry III*, Elsevier, 2007, pp. 557–601.

11 For Alder-ene cyclization of ene-allenes at 120 °C see: (*a*) K. Närhi, J. Franzén and J.-E. Bäckvall, *J. Org. Chem.*, 2006, **71**, 2914–2917. For allene-ene cyclization see: (*b*) K. K.-Y. Kung, V. K.-Y. Lo, H.-M. Ko, G.-L. Li, P.-Y. Chan, K.-C. Leung, Z. Zhou, M.-Z. Wang, C.-M. Che and M.-K. Wong, *Adv. Synth. Catal.*, 2013, **355**, 2055–2070; (*c*) M.-Z. Wang, C.-Y. Zhou, Z. Guo, E. L.-M. Wong, M.-K. Wong and C.-M. Che, *Chem. – Asian J.*, 2011, **6**, 812–824; (*d*) P.-J. Cai, Y. Wang, C.-H. Liu and Z.-X. Yu, *Org. Lett.*, 2014, **16**, 5898–5901; (*e*) C.-H. Liu and Z.-X. Yu, *Angew. Chem., Int. Ed.*, 2017, **56**, 8667–8671; (*f*) S. Ma, *Acc. Chem. Res.*, 2009, **42**, 1679–1688; (*g*) T. Bai, S. Ma and G. Jia, *Coord. Chem. Rev.*, 2009, **253**, 423–448; (*h*) J. Ye and S. Ma, *Acc. Chem. Res.*, 2014, **47**, 989–1000.

12 For review on non-catalyzed intramolecular Alder-ene see: (*a*) W. Oppolzer and V. Snieckus, *Angew. Chem., Int. Ed. Engl.*, 1978, **17**, 476–486. For reviews on metal-catalyzed intramolecular Alder-ene see: (*b*) I. D. G. Watson and F. D. Toste, *Chem. Sci.*, 2012, **3**, 2899–2919; (*c*) A. Marinetti, H. Julie and A. Voituriez, *Chem. Soc. Rev.*, 2012, **41**, 4884–4908.

13 For selected references on tandem allene formation/cyclization see: (*a*) T. Mandai, Y. Tsujiguchi, J. Tsuji and S. Saito, *Tetrahedron Lett.*, 1994, **35**, 5701–5704; (*b*) M. Nechab and N. Vanthuyne, *Org. Lett.*, 2012, **14**, 3974–3977; (*c*) For selected reviews see: D. Tejedor, G. Méndez-Abt, L. Cotos and F. García-Tellado, *Chem. Soc. Rev.*, 2013, **42**, 458–471; (*d*) K. K. Wang, in *Modern Allene Chemistry*, Wiley-VCH Verlag GmbH, Weinheim, Germany, 2004, pp. 1091–1126.

14 (*a*) N. Krause and A. S. Hashmi, in *Modern Allene Chemistry*, Wiley-VCH Verlag GmbH, Weinheim, Germany, 2004; (*b*) S. Ye and S. Ma, *Org. Chem. Front.*, 2014, **1**, 1210–1224.

15 S. N. Kessler and J.-E. Bäckvall, *Angew. Chem., Int. Ed.*, 2016, **55**, 3734–3738.

16 Y. Zhao and D. G. Truhlar, *Theor. Chem. Acc.*, 2008, **120**, 215–241.

17 For DFT a computational study of intermolecular Alder-ene reaction, see: I. Fernandez and F. M. Bickelhaupt, *J. Comput. Chem.*, 2012, **33**, 509–516.

18 For a recent review on HAT see: M. Nechab, S. Mondal and M. P. Bertrand, *Chem. – Eur. J.*, 2014, **20**, 16034–16059.

19 (*a*) D. Samanta, M. E. Cinar, K. Das and M. J. Schmittel, *Org. Chem.*, 2013, **78**, 1451–1462; (*b*) M. E. Cinar, C. Vavilala, R. Jaquet, J. W. Bats and M. Schmittel, *Eur. J. Org. Chem.*, 2014, 5166–5177; (*c*) For a more general overview see: R. K. Mohamed, P. W. Peterson and I. V. Alabugin, *Chem. Rev.*, 2013, **113**, 7089–7129.

20 K. Yamaguchi, F. Jensen, A. Dorigo and K. N. Houk, *Chem. Phys. Lett.*, 1988, **149**, 537–542.

21 The imaginary frequency for the transition state is 2250 cm^{-1} (according to Wigner's approximation, the rate constant for the hydrogen atom transfer should be increased by a factor 7, see: E. Wigner, *Z. Phys. Chem., Abt. B*, 1932, **19**, 203–216. For selected examples of studies of tunneling in hydrogen transfer isomerizations, see: (*a*) B. Sirjean, E. Dames, H. Wang and W. Tsang, *J. Phys. Chem. A*, 2012, **116**, 319–332; (*b*) A. C. Davis and

J. S. Francisco, *J. Phys. Chem. A*, 2011, **115**, 2966–2977. For a very recent discussion of the importance of the concept, see: (*c*) P. R. Schreiner, *J. Am. Chem. Soc.*, 2017, **139**, 15276–15283.

22 For the evaluation of the M06-2X functional regarding the overestimation of the free energy of activation barrier of pericyclic reactions, see: (*a*) T. R. Ramadhar and R. A. Batey, *Comput. Theor. Chem.*, 2011, **976**, 167–182; (*b*) Y. Lan, L. Zou, Y. Cao and K. N. Houk, *J. Phys. Chem. A*, 2011, **115**, 13906–13920.

23 No significant difference in activation parameters was observed for the concerted pathways going through the diastereomeric transition structures (0.003 kcal mol^{-1}).

24 For selected reports on enantioselective synthesis of indenes see: (*a*) A. Martínez, P. García-García, M. A. Fernández-Rodríguez, F. Rodríguez and R. Sanz, *Angew. Chem., Int. Ed.*, 2010, **49**, 4633–4637; (*b*) K. Takeda, T. Oohara, M. Anada, H. Nambu and S. Hashimoto, *Angew. Chem., Int. Ed.*, 2010, **49**, 6979–6983; (*c*) D. N. Tran and N. Cramer, *Angew. Chem., Int. Ed.*, 2011, **50**, 11098–11102; (*d*) S. Reddy Chidipudi, D. J. Burns, I. Khan and H. W. Lam, *Angew. Chem., Int. Ed.*, 2015, **54**, 13975–13979.

25 D. Mouysset, C. Tessonnier, A. Tintaru, F. Dumur, M. Jean, N. Vanthuyne, M. P. Bertrand, D. Siri and M. Nechab, *Chem. – Eur. J.*, 2017, **23**, 8375–8379.